Mutational, Structural, and Kinetic Evidence for a Dissociative Mechanism in the GDP-Mannose Mannosyl Hydrolase Reaction†

Zuyong Xia,‡ Hugo F. Azurmendi,‡ Luke L. Lairson,§ Stephen G. Withers,§ Sandra B. Gabelli,|| Mario A. Bianchet,|| L. Mario Amzel,|| and Albert S. Mildvan*,‡

Department of Biological Chemistry and Department of Biophysics and Biophysical Chemistry, The Johns Hopkins University School of Medicine, 725 North Wolfe Street, Baltimore, Maryland 21205-2185, and Department of Chemistry, University of British Columbia, Vancouver, British Columbia, Canada V6T 1Z1

Received March 30, 2005; Revised Manuscript Received May 4, 2005

ABSTRACT: GDP-mannose hydrolase (GDPMH) catalyzes the hydrolysis of GDP-α-D-sugars by nucleophilic substitution with inversion at the anomeric C1 atom of the sugar, with general base catalysis by H124. Three lines of evidence indicate a mechanism with dissociative character. First, in the 1.3 Å X-ray structure of the GDPMH−Mg^{2+}−GDP·$Tris^+$ complex [Gabelli, S. B., et al. (2004) *Structure 12*, 927−935], the GDP leaving group interacts with five catalytic components: R37, Y103, R52, R65, and the essential Mg^{2+}. As determined by the effects of site-specific mutants on k_{cat}, these components contribute factors of 24-, 100-, 309-, 24-, and $\geq 10^5$-fold, respectively, to catalysis. Both R37 and Y103 bind the β-phosphate of GDP and are only 5.0 Å apart. Accordingly, the R37Q/Y103F double mutant exhibits partially additive effects of the two single mutants on k_{cat}, indicating cooperativity of R37 and Y103 in promoting catalysis, and antagonistic effects on K_m. Second, the conserved residue, D22, is positioned to accept a hydrogen bond from the C2−OH group of the sugar undergoing substitution at C1, as was shown by modeling an α-D-mannosyl group into the sugar binding site. The D22A and D22N mutations decreased k_{cat} by factors of $10^{2.1}$ and $10^{2.6}$, respectively, for the hydrolysis of GDP-α-D-mannose, and showed smaller effects on K_m, suggesting that the D22 anion stabilizes a cationic oxocarbenium transition state. Third, the fluorinated substrate, GDP-2F-α-D-mannose, for which a cationic oxocarbenium transition state would be destabilized by electron withdrawal, exhibited a 16-fold decrease in k_{cat} and a smaller, 2.5-fold increase in K_m. The D22A and D22N mutations further decreased the k_{cat} with GDP-2F-α-D-mannose to values similar to those found with GDP-α-D-mannose, and *decreased* the K_m of the fluorinated substrate. The choice of histidine as the general base over glutamate, the preferred base in other Nudix enzymes, is not due to the greater basicity of histidine, since the pK_a of E124 in the active complex (7.7) exceeded that of H124 (6.7), and the H124E mutation showed a $10^{2.2}$-fold *decrease* in k_{cat} and a 4.0-fold increase in K_m at pH 9.3. Similarly, the catalytic triad detected in the X-ray structure (H124- - -Y127- - -P120) is unnecessary for orienting H124, since the Y127F mutation had only 2-fold effects on k_{cat} and K_m with either H124 or E124 as the general base. Hence, a neutral histidine rather than an anionic glutamate may be necessary to preserve electroneutrality in the active complex.

GDP-mannose mannosyl hydrolase (GDPMH)[1] catalyzes hydrolysis of nucleotide sugars such as GDP-α-D-mannose, yielding GDP and β-D-mannose (reviewed in ref *1*). The biological function of GDPMH in the bacterial cell is likely the regulation of the level of GDP-mannose which provides mannosyl components for cell wall biosynthesis, and is also an intermediate in the biosynthesis of other glycosyl donors for the cell walls of Gram-negative bacteria (*2*). GDMPH belongs to the Nudix superfamily of enzymes, defined by their ability to catalyze the hydrolysis of nucleoside diphosphate−X derivatives, and by the presence of the 23-residue Nudix box sequence, **G**X_5**E**X_7**RE**U**X**E**E**X**G**U (U = I, L, or V), which forms a loop−helix−loop structure at the active site (*1*). The bold residues are conserved, and generally play significant roles in catalysis.

Members of the GDPMH subfamily differ in at least three ways from other Nudix enzymes. First, the Nudix box sequence, **G**X_5**E**X_7**R**UX_3**E**X**G**U, lacks two Glu residues, both of which function as metal ligands in the prototypical

† This research was supported by National Institutes of Health Grants DK28616 (to A.S.M.) and GM066895 (to L.M.A.) and by the Natural Sciences and Engineering Research Council of Canada (to S.G.W.). L.L.L. is the recipient of a Natural Sciences and Engineering Research Council of Canada PGSD and a Michael Smith Foundation for Health Research Senior Graduate Studentship.

* To whom correspondence should be addressed. Phone: (410) 955-2038. Fax: (410) 955-5759. E-mail: mildvan@jhmi.edu.

‡ Department of Biological Chemistry, The Johns Hopkins University School of Medicine.

§ University of British Columbia.

|| Department of Biophysics and Biophysical Chemistry, The Johns Hopkins University School of Medicine.

[1] Abbreviations: GDPMH, GDP-mannose hydrolase; GDP-2F-α-D-mannose, guanosine 5′-(disodium diphosphate), *P*′-(2-deoxy-2-fluoro-α-D-mannopyranosyl) ester; HSQC, heteronuclear single-quantum coherence; SDS−PAGE, sodium dodecyl sulfate−polyacrylamide gel electrophoresis; AEBSF, 4-(2-aminoethyl)benzenesulfonyl fluoride hydrochloride; DTT, dithiothreitol; BCA, bicinchoninic acid; MOPS, 3-(*N*-morpholino)propanesulfonic acid; PCR, polymerase chain reaction.

10.1021/bi050583v CCC: $30.25
Published on Web 06/01/2005

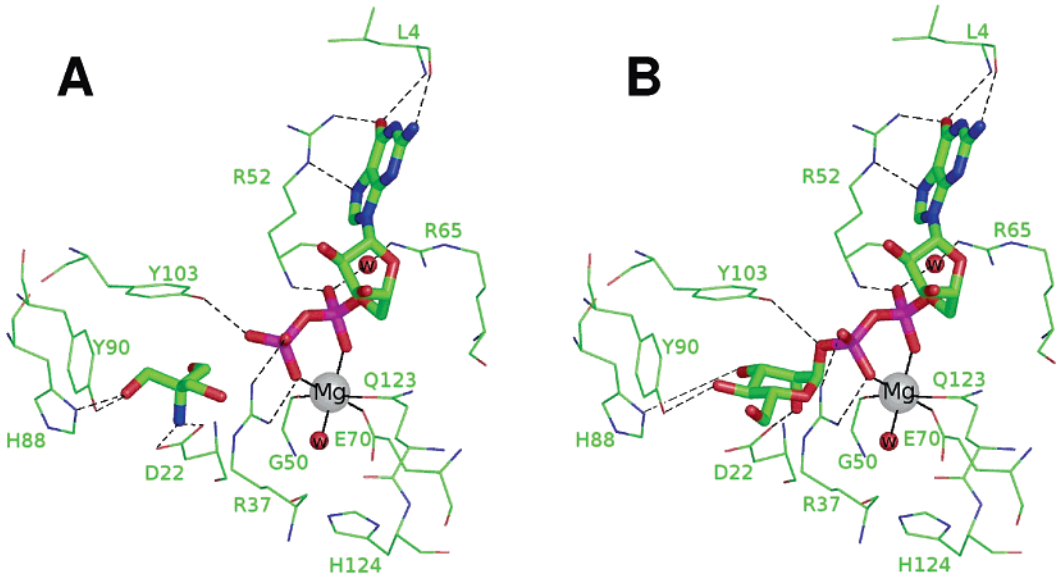

FIGURE 1: Residues at the active site of GDP-α-D-mannose hydrolase. (A) X-ray structure at 1.3 Å resolution of the enzyme−Mg^{2+}−GDP·$Tris^+$ complex in which $Tris^+$ occupies the sugar binding site (*6*). (B) Modeling of the bound substrate GDP-α-D-mannose by replacing $Tris^+$ with an α-D-mannosyl group, and energy minimization (*6*). Hydrogen bonds are represented by dashed lines.

Nudix enzyme, the MutT pyrophosphohydrolase (*3*), consistent with the order of magnitude lower affinity of GDPMH for divalent cations (*4*). Second, unlike all other well-studied Nudix enzymes which use glutamate as a general base (*1*), GDPMH uses a histidine residue, H124 (*5*), which is conserved only among members of the GDPMH subfamily (*6*). Three explanations for this difference have been considered (*1*, *6*). Histidine is more basic than glutamate; it is more easily oriented by hydrogen bond acceptors as in a catalytic triad, and a neutral histidine rather than an anionic glutamate may be required to preserve electroneutrality in the active complex.

Third, GDPMH and other Nudix enzymes differ in the site of nucleophilic substitution. While Nudix enzymes generally catalyze nucleophilic substitutions (by water) at *phosphorus* on the basis of their reaction products, and from studies of ^{18}O incorporation (*1*), the GDPMH-catalyzed hydrolysis of GDP-α-sugars involves nucleophilic substitution at the anomeric C1 atom of the sugar, with inversion (*7*). The recently determined 1.3 Å X-ray structure of the GDPMH−Mg^{2+}−GDP·$Tris^+$ complex (in which a $Tris^+$ molecule occupies the sugar binding site) (Figure 1A) has suggested an explanation for this change in the site of substitution (*6*). The bound substrate, GDP-α-D-mannose, was modeled into the active site by replacing $Tris^+$ with D-mannose in an α-linkage to the bound GDP, followed by energy minimization (Figure 1B) (*6*). The resulting structure of the GDPMH−Mg^{2+}−GDP-α-D-mannose complex was then superimposed onto that of the ADP-ribose pyrophosphatase−Mg^{2+}−ADP-ribose complex, a more conventional Nudix hydrolase which catalyzes substitution at the nucleotide α-phosphorus of an NDP-sugar (*8*). This superposition revealed that the change in the site of substitution could be ascribed to a six-residue deletion in a loop of GDPMH which shifts the location of the general base and its associated water by ~6 Å along the bound nucleotide sugar, from a position approaching the α-phosphorus to one approaching the anomeric C1 atom of the sugar (*6*). This structural difference may explain how a Nudix enzyme, which makes use of catalysis by approximation, might have evolved from one which substitutes at phosphorus to one which substitutes at carbon (*6*). However, since glycosyl transfer reactions frequently have dissociative mechanisms (*9*−*11*) while substitutions at internal phosphorus atoms are likely to be associative (*3*, *12*, *13*), other structural differences may also contribute to this change in target.

Figure 1B shows residues interacting with GDP-α-D-mannose in the active site of GDPMH as modeled from the 1.3 Å X-ray structure of the GDPMH−Mg^{2+}−GDP·$Tris^+$ complex (*6*). Consistent with prior kinetic, EPR, NMR, and mutational studies in solution which were guided by mechanistic considerations and homology with other Nudix enzymes (*4*, *5*, *7*), the X-ray structure detected a metal bridge from the enzyme to the GDP leaving group, and five catalytic residues (*6*). These were E70 (a metal ligand), H124 (the general base), R52 (which interacts with the guanine ring and the α-phosphate of GDP), R65 [which interacts with the α-phosphate (via a water)], and H88 (which accepts a hydrogen bond from an OH of the $Tris^+$ and presumably from the mannose moiety of the substrate). In addition, the X-ray structure found three new candidate catalytic residues, R37, Y103, and D22, near the reaction center phosphoglycosyl group of the bound substrate which were not anticipated by previous homology searches.

This paper describes the catalytic contributions and mechanistic roles of these newly detected active site residues, as revealed by site-directed mutagenesis. The reason for the choice of histidine rather than glutamate as the general base is also investigated by mutagenesis. These studies, and kinetic studies with a fluorinated substrate, GDP-2-deoxy-2-fluoro-α-D-mannose, similar to those used in probing glycosidase mechanisms (*14*, *15*), indicate that GDPMH has a glycosidase-like mechanism with dissociative character. A preliminary abstract of this work has been published (*16*).

EXPERIMENTAL PROCEDURES

Materials. Nucleotides GDP, GDP-α-D-mannose, and GDP-β-L-fucose were purchased from Sigma. The nucleotides and buffers were passed over Chelex-100 resin to

remove trace metal contaminants. SigmaUltra ammonium sulfate and mannosamine were also purchased from Sigma (St. Louis, MO). Enzyme-grade MOPS buffer and DTT were purchased from Fisher Scientific (Fair Lawn, NJ). Ultrapure (99.995%) $MgCl_2$ hexahydrate was purchased from Aldrich Chemical Co. (Milwaukee, WI). Ultrafiltration concentrators (polyethersulfone membrane, 10 000 molecular weight cutoff) were purchased from Vivascience (Gloucestershire, U.K.). Ecolite(+) scintillation cocktail was from ICN Biomedicals, Inc. (Costa Mesa, CA). *Escherichia coli* strain DH-5α was purchased from Gibco BRL (Grand Island, NY). *E. coli* strain BL-21(DE3) and QuikChange site-directed mutagenesis kits were purchased from Stratagene (La Jolla, CA). Plasmid DNA purification kits were purchased from Qiagen (Valencia, CA). GDP-α-D-mannose, labeled with ^3H in the C2 position of the mannose, was purchased from Perkin-Elmer (Boston, MA). The tritiated GDP-mannose was supplied in 70% ethanol and was lyophilized before being used. $^{15}NH_4Cl$ (99%) was purchased from Cambridge Isotope Labs, Inc. (Andover, MA). Calf intestinal alkaline phosphatase was purchased from New England Biolabs Inc. (Beverly, MA). Deoxymannojirimycin was purchased from Toronto Research Chemicals Inc. (North York, ON). Tris-d_{11}-HCl was purchased from Isotec Inc. (Miamisburg, OH).

Synthesis of GDP-2F-α-D-Mannose. GDP-2F-α-D-mannose was prepared by treatment of bis(triethylammonium) 2-deoxy-2-fluoro-α-D-mannopyranosyl phosphate with 4-morpholine-*N,N′*-dicyclohexylcarboxamidinium guanosine 5′-monophosphomorpholidate as described previously (*17*). ^1H, ^{31}P, and ^{19}F NMR spectra and electrospray ionization mass spectroscopic data were consistent with those reported previously (*18*).

General Methods. E. coli strain DH-5α was used for subcloning. The construction of the wild-type petGDPMH plasmid and purification of the GDPMH enzyme were described previously (*2*, *7*). *E. coli* strain BL-21(DE3), used for protein expression, was grown in MOPS medium (*7*) with ammonium chloride in the presence of 100 μg/mL ampicillin at 37 °C. The R37Q, D22A, and D22N mutants expressed insoluble protein when induced at 37 °C for 2 h and soluble protein when induced at 16 °C for 20 h. The enzymes used in these experiments were additionally desalted on a G-25 Sephadex column (22 cm × 1 cm) to remove EDTA which was present in the buffers used in the purification protocol (*7*).

After the G-50 Sephadex, DEAE-Sepharose, and G-25 Sephadex columns, all other enzymes were judged to be at least 95% pure on the basis of SDS−PAGE and Coomassie-stained gels. All of the mutants eluted as ∼36 kDa dimers from a calibrated G-50 Sephadex column like the wild-type enzyme. Before and after desalting had been carried out, the enzyme was concentrated using Vivaspin ultrafiltration concentrators. The concentration of GDPMH was determined spectrophotometrically using an ϵ_{280}^{native} of 72.8 mM^{-1} cm^{-1} at pH 6.5 in 20 mM phosphate buffer (*19*) and by the BCA assay using BSA as the standard (*4*). The two methods differed by 3% for the GDPMH protein. The concentrations of GDP and GDP-α-D-mannose were determined using an $\epsilon_{252.5}$ of 13.6 mM^{-1} cm^{-1} at pH 6.0 in 50 mM MES buffer.

Preparation of GDPMH Mutants. Mutagenesis was carried out as previously described (*5*, *20*). The sequences of coding and complementary noncoding mismatch primers used for the mutations are as follows: R37Q, 5′-TTT CTG CTT GGC AAA CAG ACC AAC CGC CCG GCG-3′ and 5′-CGC CGG GCG GTT GGT CTG TTT GCC AAG CAG AAA-3′; Y103F, 5′-GAT TTC ACC ACT CAC TTT GTG GTG CTC GGT TTT-3′ and 5′-AAA ACC GAG CAC CAC AAA GTG AGT GGT GAA ATC-3′; H124E, 5′-CTG CCG GAT GAG CAG GAA GAC GAT TAC CGC TGG-3′ and 5′-CCA GCG GTA ATC GTC TTC CTG CTC ATC CGG CAG-3′; D22A, 5′-CCG CTT GTC TCT CTC GCA TTT ATT GTC GAG AAC-3′ and 5′-GTT CTC GAC AAT AAA TGC GAG AGA GAC AAG CGG-3′; D22N, 5′-CCG CTT GTC TCT CTC AAC TTT ATT GTC GAG AAC-3′ and 5′-GTT CTC GAC AAT AAA GTT GAG AGA GAC AAG CGG-3′; and Y127F, 5′-CGA CGT CAG CCA GCG AAA ATC GTC ATG CTG CTC-3′ and 5′-GAG CAG CAT GAC GAT TTT CGC TGG CTG ACG-3′.

Each coding strand primer and noncoding strand primer was complementary to the noncoding strand, except at the appropriate mismatch (underlined) in the codon designating the amino acid to be mutated. The wild-type GDPMH gene in the pET11b vector was used as the template for the PCR to generate the single mutants of GDPMH, following the instruction manual of the QuickChange site-directed mutagenesis kit. For preparation of the R37Q/Y103F and H124E/Y127F double mutants, the single mutant plasmids pETGDPMH-R37Q and pETGDPMH-H124E were used as the templates and the Y103F and Y127F coding and noncoding mismatch DNA oligonucleotides (see above) were used as the primers in the PCR, respectively. The PCR protocol consisted of a hot start at 95 °C for 30 s and 16 cycles; one cycle consisted of denaturation at 95 °C for 30 s, annealing at 55 °C for 60 s, and elongation at 68 °C for 12 min. After 16 cycles, the reaction mixtures were kept at 4 °C. The plasmid was subcloned into DH-5α *E. coli* cells. The plasmid DNA was then purified using the Qiagen miniprep kit and then cloned into BL-21(DE3) *E. coli* cells for protein expression. All plasmids containing inserts were isolated and sequenced to verify the mutation and the otherwise unaltered DNA sequence.

GDPMH Assay. The assay used to measure the extent of hydrolysis of GDP-α-D-mannose was previously described (*4*, *5*). Briefly, the production of GDP during the course of the reaction was followed by measuring the concentration of phosphate produced upon treatment of the GDP product with calf intestinal alkaline phosphatase in a coupled enzyme assay. Alkaline phosphatase does not affect the GDP-α-D-mannose substrate. Mutants were assayed at 37 °C and pH 9.3 for 15−20 min after initiating the reaction with 1−2 milliunits of enzyme. Other components that were present were 80 mM Na^+ glycine buffer (pH 9.3), 20 mM $MgCl_2$, and 1 unit of calf intestinal alkaline phosphatase in a total volume of 50 μL. The reactions were terminated by adding 250 μL of 5.0 mM Na^+ EDTA followed by 700 μL of Ames Mix (6 parts 0.42% ammonium molybdate in 1 N H_2SO_4 and 1 part 10% ascorbic acid). After incubation for 30 min at 37 °C, the optical density was measured at 780 nm (*2*, *7*). The low activities of the R37Q, D22A, and D22N mutants were measured using GDP-α-D-mannose as the substrate, tritiated at the C2′ position of the mannose, as described previously (*4*).

Effect of pH on the k_{cat} of the H124E Mutant. The pH dependence of k_{cat} was determined at eight pH values over

the range of 6.0−9.5 as described previously (*5*), using 80 mM Na^+ MES buffer for pH values between 6.0 and 7.0, 80 mM Tris-HCl for pH values between 7.0 and 8.5, and 80 mM Na^+ glycine for pH values between 8.5 and 9.5. The pH values of all assays were checked in parallel samples. Two concentrations of the substrate, 5.0 and 10.0 mM GDP-α-D-mannose, were used to ensure saturation at each pH. Other components that were present were 20.0 mM $MgCl_2$, 1.0 unit of calf intestinal alkaline phosphatase, and 2.5 milliunits of the H124E mutant enzyme in a total volume of 50 μL. The reactions were terminated at 15 min as described above, except that Ames Mix was replaced by a solution containing 1 part 34 mM $(NH_4)_6Mo_7O_{24}$ in 5.0 M HCl and 3 parts 2.16 mM malachite green oxalate, to enhance the detection of phosphomolybdate because of its greater sensitivity (*21*). The data were fit to the logarithmic form of eq 1 by nonlinear least-squares methods to obtain the pK_a of E124, as previously described (*22*).

$$k_{cat} = (k_{cat})^{max}/(1 + [H^+]/K_{HES}) \quad (1)$$

Inhibition Studies. For the measurement of the K_I^{slope} of GDP-β-L-fucose, assays were carried out at 37 °C in 80 mM Na^+ HEPES buffer (pH 7.2). The lower pH was used to prevent high background rates found with substrates other than GDP-α-D-mannose. Other components that were present were GDP-α-D-mannose (0.13, 0.26, 0.51, 0.77, and 1.28 mM), GDP-β-L-fucose (0.0, 0.09, and 0.26 mM), $MgCl_2$ (20 mM), and 1.0 μg of GDPMH in a total volume of 50 μL. Inhibition studies with the cationic sugar analogues mannosamine, deoxymannojirimycin, and $Tris^+$ were carried out using 1.0 mM GDP-α-D-mannose as the substrate, in the absence or presence of GDP (80 μM), under conditions otherwise identical to those used for inhibition by GDP-β-L-fucose.

NMR Studies. As previously described (*5*), mutant enzymes were examined for structural changes by comparing their two-dimensional $^1H-^{15}N$ HSQC spectra with that of the wild-type enzyme. The number of resonances with changes in chemical shifts of ≥0.5 ppm in the ^{15}N dimension and ≥0.05 ppm in the proton dimension were counted. Although the backbone and side chain ^{15}N and NH resonances of this asymmetric homodimer have not yet been assigned, changes in their chemical shifts provide a sensitive phenomenological measure of structural changes (*5*). NMR spectra were obtained at 30 °C on a Varian INOVA 600 MHz NMR spectrometer equipped with a pulse field gradient unit and a triple-resonance, actively shielded z-gradient probe. NMR samples contained 1.0 mM enzyme subunits, 4.0 mM Tris-d_{11}-HCl (pH 7.5), 21 mM NaCl, 10 mM DTT, 0.3 mM NaN_3, 0.1 mg/mL AEBSF, and 10% D_2O.

RESULTS

Kinetic Studies of R37 and Y103 Mutants. R37 and Y103 are not located in the Nudix sequence of GDPMH (residues 51−73), nor are they conserved throughout the entire Nudix superfamily of enzymes. However, R37 and Y103 are conserved in the GDPMH subfamily of Nudix enzymes found in *Enterobacteria* and *Vibrio* (*6*). The crystal structure (Figure 1) reveals that R37 is positioned well to interact electrostatically and to donate hydrogen bonds (2.82 and 3.09 Å) to the β-phosphate of the GDP moiety of the cleaved phosphoglycosyl bond. Mutation of R37 to Q resulted in a 24-fold decrease in k_{cat} and an 8.5-fold increase in the K_m of GDP-α-D-mannose (Table 1), suggesting that R37 plays an important role in catalysis by helping to stabilize the β-phosphate of the leaving GDP. Similarly, Y103 donates a hydrogen bond (O- - -O distance of 2.59 Å) to the leaving oxygen in the phosphoglycosyl bond. The Y103F mutation led to a 100-fold decrease in k_{cat} and a 6.9-fold increase in K_m, suggesting that this hydrogen bond also makes a significant contribution to catalysis.

Table 1: Kinetic Constants of Wild Type GDPMH and Mutants at pH 9.3 and 37 °C with Mg^{2+} Activation and GDP-α-D-Mannose as the Substrate

enzyme	k_{cat} (s^{-1})	$K_m^{GDP-mannose}$ (mM)	*x*-fold change in k_{cat}	*x*-fold change in $K_m^{GDP-mannose}$
wild-type	0.33 ± 0.024	0.67 ± 0.15	1.0	1.0
R37Q	0.0138 ± 0.00105	5.7 ± 1.4	$10^{-1.4}$	8.5
Y103F	0.0032 ± 0.00028	4.6 ± 1.0	$10^{-2.0}$	6.9
R37Q/Y103F	0.00175 ± 0.00052	3.0 ± 0.6	$10^{-2.3}$	4.4
D22A	0.0027 ± 0.0001	3.0 ± 0.3	$10^{-2.1}$	4.5
D22N	0.00080 ± 0.00015	5.8 ± 2.6	$10^{-2.6}$	8.7
H124E	0.0020 ± 0.00015	2.7 ± 0.7	$10^{-2.2}$	4.0
Y127F	0.180 ± 0.007	0.33 ± 0.05	0.55	0.49
H124E/Y127F	0.0058 ± 0.0004	2.3 ± 0.3	$10^{-1.8}$	3.4

Side chain Nη of R37 and Oη of Y103 are only 5.0 Å apart, and both residues interact with different oxygens of the leaving β-phosphate, suggesting that these residues might act cooperatively to promote catalysis. Accordingly, the R37Q/Y103F double mutant exhibited an only 200-fold decrease in k_{cat}, 12-fold lower than the product of the effects of the two single mutants (2400-fold), indicating only partial additivity of their damaging effects on k_{cat} in the double mutant (*23*, *24*). Such partial additivity indicates partially cooperative contributions of R37 and Y103 to catalysis, with the cooperative component contributing a factor of 12 to the total effect of each single mutation, as measured by the 12-fold departure from additivity. Once one corrects for this cooperative component, the intrinsic, noncooperative contributions of R37 and Y103 to k_{cat} are 2- and 8.3-fold, respectively. Stated inversely by using the double mutant as the point of reference (*24*), the k_{cat} of the double mutant is decreased 200-fold. Restoring only R37 (as in the Y103F mutant) increases k_{cat} by 2-fold. Restoring only Y103 (as in the R37Q mutant) increases k_{cat} by 8.3-fold. Restoring both R37 and Y103, as in the wild type, increases k_{cat} by 200-fold, directly measuring the cooperative contribution to catalysis as the extra factor of 12 (equivalent to 1.45 kcal/mol).

The R37Q/Y103F double mutant exhibited an only 4.4-fold increase in K_m, a less damaging effect than that found with either the R37Q single mutant (8.5-fold) or the Y103F single mutant (6.9-fold). These factors indicate reciprocal, antagonistic effects of the Y103F and R37Q mutations on the K_m values, presumably resulting from opposing structural effects which permit the double mutation to partially repair the damage to K_m caused by either single mutation (*23*). The product of the effects on K_m of the two single mutations exceeds the effect of the double mutant by a factor of 13 (equivalent to 1.50 kcal/mol), providing a quantitative

Table 2: Kinetic Parameters of Wild-Type GDPMH and Mutants at pH 7.2 and 37 °C with Mg^{2+} Activation and Various Substrates[a]

enzyme	substrate	k_{cat} (s^{-1})	$K_m^{GDP-sugar}$ (mM)	*x*-fold change in k_{cat}	*x*-fold change in $K_m^{GDP-sugar}$
wild type	GDP-α-D-mannose	0.28 ± 0.009	0.30 ± 0.03	1.0	1.0
	GDP-α-D-glucose	1.19 ± 0.08	0.87 ± 0.19	4.3	2.9
	GDP-2F-α-D-mannose	0.0174 ± 0.0037	0.76 ± 0.29	$10^{-1.2}$	2.5
	GDP-β-L-fucose	0.0048 ± 0.0001	0.046 ± 0.007	$10^{-1.8}$	0.15
D22A	GDP-α-D-glucose	0.0028 ± 0.0005	3.7 ± 1.2	$10^{-2.6}$	4.3
	GDP-2F-α-D-mannose	0.0039 ± 0.0003	0.44 ± 0.10	0.22	0.58
	GDP-β-L-fucose	0.00068 ± 0.00006	0.23 ± 0.05	0.14	5.0
D22N	GDP-α-D-glucose	0.00068 ± 0.00009	2.2 ± 0.7	$10^{-3.2}$	2.5
	GDP-2F-α-D-mannose	0.00037 ± 0.00003	0.26 ± 0.09	$10^{-1.7}$	0.34
	GDP-β-L-fucose	0.00012 ± 0.00001	0.22 ± 0.07	$10^{-1.6}$	4.8

[a] Parameters of substrates with wild-type GDPMH are compared to those of GDP-α-D-mannose. Parameters of mutants are compared to those of wild-type GDPMH with the same substrate.

measure of the antagonism between the two residues on the basis of their influence on K_m.[2]

$^1H-^{15}N$ HSQC Spectrum of the R37Q/Y103F Double Mutant. Comparison of the $^1H-^{15}N$ HSQC spectrum of the R37Q/Y103F double mutant with that of the wild-type enzyme showed that only seven cross-peaks of 172 shifted by more than 0.5 ppm in the ^{15}N dimension, and only 15 shifted by more than 0.05 ppm in the proton dimension, indicating little structural change.

Kinetic Studies of D22 Mutants. D22, a residue conserved only in the GDPMH subfamily of Nudix enzymes, is found in the $Tris^+$ (sugar) binding site where both of its δ oxygens accept hydrogen bonds (2.81 and 3.08 Å) from the $Tris^+$ nitrogen (*6*), suggesting that D22 is anionic. In the modeled GDPMH−Mg^{2+}−GDP-α-D-mannose complex (Figure 1B), a carboxylate oxygen of D22 is positioned well to accept a hydrogen bond from the axial 2-OH of the mannose (*6*). With GDP-α-D-mannose as substrate, the D22A mutant showed a 122-fold decrease in k_{cat} and a 4.5-fold increase in K_m (Table 1). The isoelectronic D22N mutation decreased k_{cat} 413-fold and increased K_m 8.7-fold, indicating an important role in catalysis of the D22 anion.

When the substrate GDP-α-D-glucose is used (Table 2), in which the 2-OH of the hexose is equatorial rather than axial, wild-type GDPMH exhibited a 4.3-fold increase in k_{cat} and a 2.9-fold increase in K_m, with respect to those of GDP-α-D-mannose. With GDP-α-D-glucose, the D22A and D22N mutations decreased k_{cat} 425- and 1750-fold, respectively, and increased the K_m values by factors of 4.4 and 2.5, respectively. The larger effects of the D22 mutations on k_{cat} than on K_m with both substrates (Tables 1 and 2) indicate a predominantly catalytic rather than a substrate binding role for the D22 anion. The similar effects of the D22 mutations on the kinetic parameters of both GDP-α-D-mannose (Table 1) and GDP-α-D-glucose (Table 2) are consistent with the interaction of D22 with the 2-OH group of the hexose as shown in the structure-based model (Figure 1B). In this location, the anionic D22 is also positioned well to stabilize a cationic oxocarbenium transition state in a dissociative mechanism, similar to those proposed for glycosidases (*9*−*11*). In glycosidase mechanisms, an anionic glutamate or aspartate residue near the 2-OH of the sugar which is undergoing substitution at C1 plays significant roles in the geometric and electrostatic stabilization of the transition state (*9*−*11*).

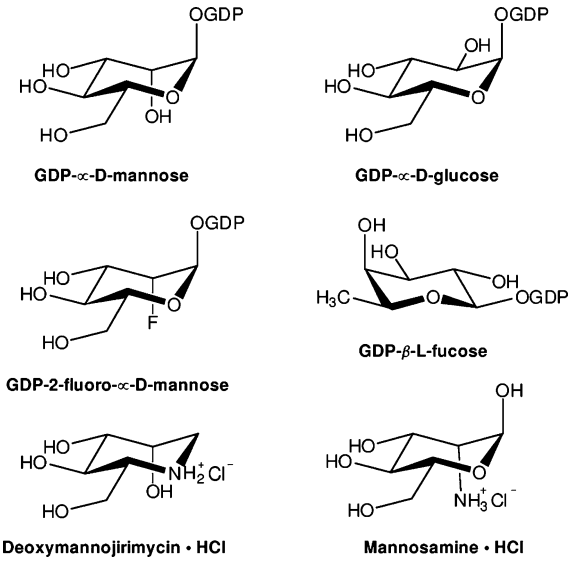

FIGURE 2: Structures of substrates and inhibitors used in these studies.

$^1H-^{15}N$ HSQC Spectra of D22 Mutants. The $^1H-^{15}N$ HSQC spectrum of the D22A mutant showed better resolution in the presence of 10 mM $MgCl_2$ and 2.0 mM GDP. Comparison of this spectrum with that of the wild-type enzyme under identical conditions showed that only eight cross-peaks of 172 shifted by more than 0.5 ppm in the ^{15}N dimension, and only 21 shifted by more than 0.05 ppm in the proton dimension. The $^1H-^{15}N$ HSQC spectrum of the D22N mutant showed that only 12 of 155 resolved cross-peaks shifted by more than 0.5 ppm in the ^{15}N dimension, and 23 shifted by more than 0.05 ppm in the proton dimension from those of the wild-type enzyme, suggesting only small structural changes.

Substrate Properties of GDP-2F-α-D-Mannose. Fluorinated sugars have long been used as alternative substrates and inhibitors to probe enzyme mechanisms (*14*, *15*). GDP-2F-α-D-mannose, in which the 2-OH group of the mannose has been replaced with fluorine (Figure 2), cannot donate a hydrogen bond to D22. Further, the presence of the fluorine would destabilize an oxocarbenium ion-like transition state by electron withdrawal. With wild-type GDPMH, the substrate GDP-2F-α-D-mannose exhibits significantly lower activity than GDP-α-D-mannose, with a 16-fold decrease in

[2] Stated inversely (24), the R37Q/Y103F double mutant, which shows a 4.4-fold increase in K_m, is used as the reference. Restoring only R37 (as in the Y103F mutant) further increases K_m by 1.6-fold. Restoring only Y103 (as in the R37Q mutant) further increases K_m by 1.9-fold. Restoring both residues, as in the wild type, antagonistically *decreases* K_m by a factor of 1/4.4-fold, an effect which is 13-fold lower than the product of the effects of the two single mutations ($1.6 \times 1.9 = 3.0$).

Table 3: Inhibitors of the Hydrolysis of GDP-α-D-Mannose by Wild-Type GDPMH at pH 7.2 and 37 °C with Mg^{2+} Activation

inhibitor	type of inhibition	K_I (mM)
GDP	competitive	0.056 ± 0.023[a]
GDP-β-L-fucose	competitive	0.019 ± 0.001
GDP-2F-α-D-mannose	competitive[b]	1.7 ± 0.1
deoxymannojirimycin$^+$	competitive	33 ± 11
deoxymannojirimycin$^+$ and GDP	competitive	13 ± 5
mannosamine$^+$	competitive	≥ 49
mannosamine$^+$ and GDP	competitive	23 ± 11
Tris$^+$	competitive[b]	≥ 140

[a] From ref *4*. [b] Assumed to be competitive with respect to GDP-α-D-mannose.

k_{cat} and a 2.5-fold greater K_m of 0.76 mM (Table 2). GDP-2F-α-D-mannose is a linear competitive inhibitor of the hydrolysis of GDP-α-D-mannose with a K_I (1.7 mM) comparable to its K_m as a substrate (Table 3).

With GDP-2F-α-D-mannose as the substrate, the D22A and D22N mutations further decreased k_{cat} with respect to that of the wild-type enzyme by factors of 4.5- and 47-fold, respectively (Table 2). The resulting k_{cat} values are similar to those found for the same mutants when GDP-α-D-mannose is used as the substrate (Table 1). This observation is consistent with further destabilization of a cationic transition state by the loss of this nearby anionic residue. Unlike the results with GDP-α-D-mannose or GDP-α-D-glucose as the substrate, where the D22A and D22N mutations *increased* the K_m (Tables 1 and 2), with GDP-2F-α-D-mannose these mutations *decreased* the K_m by factors of 1.7 and 2.9, respectively (Table 2), suggesting that the anionic D22 interacts favorably with the 2-OH group of mannose or glucose but unfavorably with the 2F group.

Substrate Properties GDP-β-L-Fucose. GDP-β-L-fucose differs in structure from GDP-α-D-mannose in four ways (Figure 2). First, the sugar is bonded to the GDP via an equatorial rather than an axial oxygen. Second, the C2−OH group is equatorial rather than axial. Third, the C4−OH group is axial rather than equatorial. Fourth, the equatorial C5−CH_2OH group is replaced by an equatorial C5−CH_3 group. It is therefore not surprising that GDP-β-L-fucose is a poor substrate of GDPMH with a k_{cat} which is 58-fold lower than that of GDP-α-D-mannose (Table 2). However, the K_m of GDP-β-L-fucose (46 μM) is 6.5-fold *lower* than that of GDP-α-D-mannose. Accordingly, GDP-β-L-fucose is a potent competitive inhibitor of the hydrolysis of GDP-α-D-mannose with a K_I of 19 ± 7 μM (Table 3). With GDP-β-L-fucose as the substrate, the D22A and D22N mutations decreased k_{cat} by factors of 7.1 and 40, respectively, and increased K_m by factors of 5.0 and 4.8, respectively (Table 2), indicating significant contributions of D22 to both sugar binding and catalysis.

Inhibition of GDPMH by Cationic Sugar Analogues. In a search of cationic sugar analogues for possible transition state analogues (Figure 2), we found only very weak inhibition at pH 7.2 by mannosamine$^+$, deoxymannojirimycin$^+$, and Tris$^+$, with K_I values (assuming competitive inhibition) of ≥49, 33, and ≥140 mM, respectively (Table 3). With deoxymannojirimycin$^+$ [pK_a = 7.35 (*25*)], raising the pH to 9.0 abolished the inhibition, suggesting the inhibition to be due to the cationic form. In the presence of GDP (80 μM) at pH 7.2, the K_I values of mannosamine$^+$ and deoxymannojirimycin$^+$ decreased slightly to 23 and 13 mM, respectively. Hence, even though these compounds, like Tris$^+$ (*6*), may bind weakly at the active site, they appear to be unable to assume the conformation of the transition state.

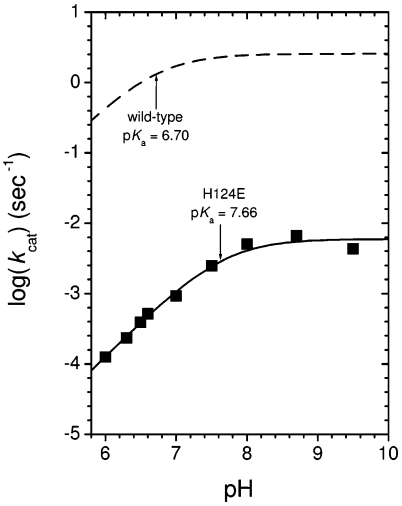

FIGURE 3: pH dependence of k_{cat} for the H124E mutant of GDPMH at 37 °C. The data are fitted to the logarithmic form of eq 1 to yield the indicated pK_a value. Experimental conditions are given in the text. The dashed curve shows the effect of pH on the k_{cat} of wild-type GDPMH, previously determined under otherwise identical conditions (*5*).

Kinetic Studies of the H124E Mutant. Unlike other Nudix enzymes, which use glutamate as the general base, GDPMH uses H124 on the basis of the approximate agreement of its pK_a of 6.94 ± 0.04 determined by direct NMR titration with the pK_a values of 6.70 ± 0.06 and 6.38 ± 0.20 determined kinetically, from the effect of pH on k_{cat} and k_{cat}/K_m, respectively (*5*). The role of H124 as general base was confirmed by the $10^{3.4}$-fold decrease in k_{cat} and the loss of the pH dependence of k_{cat} in the H124Q mutant (*5*). Moreover, the X-ray structure (*6*) and NMR studies (*1, 5*) showed H124 to be in the second coordination sphere of the essential Mg^{2+} with its unprotonated Nε approaching a metal-bound water ligand which was positioned well to add to C1 of the mannose (Figure 1).

Possible reasons for the evolutionary selection of a neutral histidine over an anionic glutamate were investigated by preparing the H124E mutant. At pH 9.3 and 37 °C, conditions under which both H124 and E124 are fully deprotonated, and with GDP-α-D-mannose as the substrate, the H124E mutant exhibited a 165-fold decrease in k_{cat} and a 4.0-fold increase in K_m, demonstrating that histidine is a much better choice (Table 1). From the effect of pH on k_{cat}, the pK_a of H124 in the active complex is 6.70 ± 0.06 (*5*), close to that of a solvent-exposed histidine (*26*). Surprisingly, the pK_a of E124 is 7.66 ± 0.07 under the same conditions (Figure 3), which is ~3.3 units (or 4.6 kcal/mol) higher than that of a solvent-exposed glutamate (*26*). Clearly, the 165-fold greater activity of wild-type GDPMH cannot be explained by the greater basicity of histidine at position 124, since the pK_a of H124 is 1.0 unit *lower* than that of E124 in their respective active complexes.

Because of the high pK_a of E124, two experiments were carried out to confirm that a glutamate, rather than a displaced nitrogen base, was functioning as the general base in the H124E mutant. First, increasing the ionic strength by

adding 0.3 mM NaCl to the assay of the H124E mutant *decreased* the kinetically determined pK_a of E124 by 0.5 unit, from 7.66 ± 0.07 to 7.16 ± 0.17, consistent with a glutamate, and the opposite of that expected for a nitrogen base (*5*). With wild-type GDPMH, the pK_a of H124 in the active complex *increased* by 0.6 unit in the presence of 0.3 M NaCl (*5*). Second, lowering the assay temperature from 37 to 8 °C did not significantly alter the pK_a of E124 in the active complex (7.66 ± 0.07 at 37 °C vs 7.62 ± 0.09 at 8 °C), consistent with a glutamate ($\Delta H_0^{ionization} = 0.0 \pm 1.5$ kcal/mol) and not with a histidine ($\Delta H_0^{ionization} = 7.2 \pm 0.3$ kcal/mol) (*26*). In the active complex of wild-type GDPMH, the pK_a of H124 *increased* with decreasing temperature, yielding a $\Delta H_0^{ionization}$ of 7.0 ± 0.7 kcal/mol (*5*).

The unusually high pK_a of E124 may result in part from the interaction of this residue in its protonated form with the noncoordinated Oϵ1 atom of the metal ligand E70, which is within hydrogen bonding distance (3.4 Å) of Oϵ1 of E124, as modeled by replacing H124 with glutamic acid in the X-ray structure (*6*).[3] In the wild-type enzyme, Nδ and Nϵ of H124 are 4.3 and 4.5 Å, respectively, from Oϵ1 of E70, too far to donate hydrogen bonds, and the N−H···O hydrogen bond angles (~90°) would be unfavorable.

The suggestion that histidine is more easily oriented than glutamate in the H124- - -Y127- - -P120 catalytic triad detected crystallographically (*6*) is unlikely, since the Y127F single mutation had little effect on catalysis, decreasing both k_{cat} and K_m by factors of ~2, and in comparison with the H124E single mutant, the H124E/Y127F double mutant antagonistically *increased* k_{cat} 2.8-fold and had no effect on K_m (Table 1). Hence, a neutral histidine rather than an anionic glutamate as a general base may be necessary to preserve electroneutrality in the active complex.[3]

^{1}H−^{15}N HSQC Spectra of the Y127F Mutant and the H124E/Y127F Double Mutant. Comparison of the ^{1}H−^{15}N HSQC spectrum of the kinetically undamaged Y127F single mutant with that of the wild-type enzyme showed that only two of 175 cross-peaks shifted by more than 0.5 ppm in the ^{15}N dimension, and only 10 shifted by more than 0.05 ppm in the proton dimension, indicating minimal structural changes. Similarly, the spectrum of the H124E/Y127F double mutant showed that only two of 175 cross-peaks shifted by more than 0.5 ppm in the ^{15}N dimension, and that only 11 shifted by more than 0.05 ppm in the proton dimension, in comparison with that of the wild-type enzyme, indicating minimal structural changes. Comparing the ^{1}H−^{15}N HSQC spectrum of the H124E/Y127F double mutant with that of the Y127F single mutant revealed only one shifted cross-peak in the ^{15}N dimension and seven in the proton dimension, indicating that the H124E mutation added little structural change to the Y127F mutant.

DISCUSSION

Kinetic and structural data provide three lines of evidence for a dissociative mechanism for the reaction catalyzed by GDPMH (Figure 4). First, there is extensive activation of the departure of the GDP leaving group with no fewer than five catalytic components involved, the essential Mg^{2+}, R37, Y103, R52, and R65 (Figures 1 and 4), which individually contribute factors from 24 to $\geq 10^5$ to k_{cat}. This is in sharp contrast with those Nudix enzymes which catalyze nucleophilic substitutions at phosphorus such as the MutT dGTP pyrophosphohydrolase, in which only a single lysine interacts with the dGMP leaving group (*3*), and with ADP-ribose pyrophosphatase, in which a Mg^{2+} and an arginine interact with the ribose 5-phosphate leaving group (*8*). Clearly, activation of the leaving group is much more important in the GDPMH reaction which involves substitution at carbon and the glycosylation of water, a reaction reminiscent of those catalyzed by inverting glycosidases where the leaving glycosidic oxygen is activated by protonation by a carboxyl group (*9*−*11*).

Second, dissociative glycosyl transfer mechanisms involve a transition state with a half-chair conformation and a planar, cationic oxocarbenium ion at C1 (Figure 4B) (*9*−*11*). The $10^{2.1}$−$10^{3.2}$-fold contribution to k_{cat} of D22, which is anionic and positioned well to stabilize a cationic transition state, and the $10^{2.3}$-fold contribution to k_{cat} of H88 (*5*), which is positioned well to accept a hydrogen bond from the C3−OH of the sugar undergoing distortion (*6*), are consistent with a dissociative transition state. Our failure to detect potent inhibition of GDPMH by cationic sugars and sugar analogues, including $Tris^+$, even in the presence of GDP, may have resulted from their inappropriate conformations which precluded tight binding. The most potent inhibitor and also the substrate with the lowest K_m was GDP-β-L-fucose, with four structural differences from α-D-mannose in the sugar ring (Figure 2). The fortuitously tight binding of GDP-β-L-fucose in its ground state may contribute to its 58-fold lower k_{cat} as a substrate.

Third, the fluorinated substrate, GDP-2F-α-D-mannose, for which a cationic oxocarbenium ion-like transition state would be destabilized by electron withdrawal (*9*, *14*, *15*), has a 16-fold lower k_{cat} than the parent substrate and a 2.5-fold higher K_m. The decrease in k_{cat} associated with fluorine substitution is quite consistent with the 50-fold decrease observed in acid-catalyzed hydrolysis rates of sugar phosphates with the analogous substitution (*28*). This is smaller than those often seen for glycosidases acting on analogous substrates, but in those cases, specific hydrogen bonding interactions involving the 2-OH group can be very important (*29*). The further decreases in k_{cat} for this substrate obtained with the D22A and D22N mutants are also consistent with a cationic transition state.

In comparing and contrasting the mechanism of GDPMH with those of glycosidases, we note that most glycosidases activate the leaving glycosidic group by protonation by a carboxyl group (*9*−*11*). In contrast, GDPMH uses five catalytic components to promote the departure of the leaving GDP: the essential Mg^{2+}, R37, Y103, R52, and R65 (Figures 1 and 4). The glycosyl oxocarbenium ion-like transition state in glycosidases is stabilized not only by means of a carboxylate anion to provide charge stabilization but also through multiple interactions with the sugar hydroxyls, thereby stabilizing the presumed half-chair conformation (*9*−*11*). GDPMH appears to use only two residues for this purpose, D22 and H88 (*5*), possibly supplemented by Y90

[3] A calculation of the electrostatic potential difference between an anionic glutamate and a neutral histidine at position 124 of GDPMH, using the program CHARMM (*27*) and the dielectric constant of water at 37 °C ($\epsilon = 74.16$), indicated that E124 is 3.1 kcal/mol less stable than H124. This electrostatic effect, together with hydrogen bond donation to E70 by the protonated form of E124, may contribute to the high pK_a of E124.

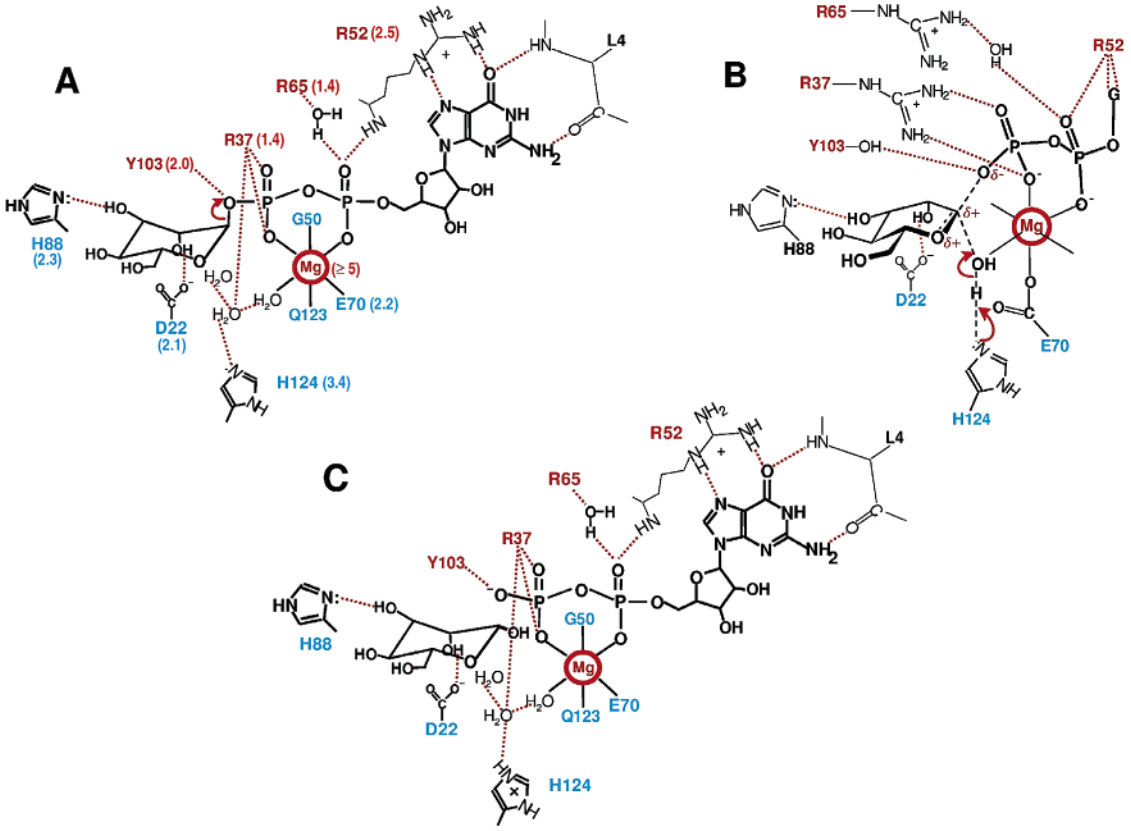

FIGURE 4: Proposed mechanism of GDP-α-D-mannose hydrolase on the basis of the work presented here and previous kinetic (*4*, *5*, *7*), stereochemical (*7*), EPR (*4*), NMR (*5*), X-ray (*6*), and mutational studies (*5*). The metal-bound water is assumed to be the entering substrate because of its fixed position and presumed lower pK_a (*6*). (A) Substrate complex showing electrophilic or Lewis acid residues labeled in red and nucleophilic or basic residues labeled in blue. Numbers in parentheses indicate the logarithms of the contributions to catalysis of individual residues, from the effects of their mutation on k_{cat}. (B) Transition state showing oxocarbenium character as discussed in the text. (C) Product complex showing inversion at C1 of the sugar (*7*). Hydrogen bonds are represented by red dotted lines.

and P41, as suggested by the X-ray structure (*6*), although these latter two residues have not been tested by mutagenesis. Consequently, much less transition state stabilization is expected. This is reflected in the fact that GDP-*β*-L-fucose, which differs greatly in structure from GDP-α-D-mannose (Figure 2), is, however, still hydrolyzed, suggesting a less highly organized sugar binding site on GDPMH than on glycosidases. It is also reflected in the much smaller (10^{12}- vs 10^{17}-fold) rate acceleration provided by GDPMH than by typical glycosidases (*5*, *30*). Poorer transition state stabilization than in glycosidases is perhaps not surprising given that this enzyme presumably evolved from a progenitor that catalyzes pyrophosphoryl transfer rather than glycosyl transfer. In that case, specific transition state stabilizing interactions would have focused around the phosphate rather than around the sugar. These effects have been noted and quantitated previously in a similar system (*31*).

Activation of the H_2O entering group may occur in mechanisms with dissociative character. With glycosidases, general base catalysis by glutamate or aspartate is generally found (*9*−*11*). With GDPMH, the deprotonation of H_2O is accomplished by the general base, H124, which is $10^{2.2}$-fold more effective than glutamate at this position (Table 1). The evolutionary selection of histidine over the glutamate found in other Nudix enzymes (*1*) is not a result of the greater basicity of histidine, since the pK_a of H124 is 1.0 unit *lower* than that of E124 in the active complex, nor is it because H124 is part of the H124- - -Y127- - -P120 catalytic triad found in the X-ray structure (*6*), since disruption of this triad by the Y127F mutation has little effect on k_{cat}. We are left with the conclusion that a neutral histidine rather than an anionic glutamate as a general base may be necessary to preserve electroneutrality at the active site.[3] Interestingly, this occurrence of neutral catalytic residues in enzymes handling anionic substrates has been seen in several cases. Examples include the sialidases, in which a nucleophilic tyrosine is employed rather than the usual glutamate or aspartate. This, coupled with a late transition state, presumably prevents electrostatic repulsion with the anionic substrate (*32*). Similarly, glycosidases in family 1 that cleave anionic thioglycoside substrates (myrosinases) uniquely have their acid/base glutamate replaced with a nonbasic glutamine, and X-ray crystallography suggests that the cofactor ascorbate, which binds at a later step, substitutes for the function of the catalytic base (*33*, *34*).

Figure 4 shows a mechanism and a transition state proposed for GDPMH on the basis of the mutational and kinetic data presented here (Tables 1 and 2) and previous structural (*4*, *6*) and mutational studies (*5*). As shown by the effects of these mutations on k_{cat} (Figure 4A), the product of the contributions to catalysis of R37 and Y103 (taking their cooperativity into account), R52, R65, Mg^{2+}, D22, H124, and H88 is $\geq 10^{19}$, which exceeds the 10^{12}-fold rate acceleration produced by GDPMH by a factor of $\geq 10^{7}$. Hence, additional pairs or groups of catalytic residues must act cooperatively to promote catalysis. These cooperative interactions can be clarified by measuring the kinetic effects of double mutations.

ACKNOWLEDGMENT

We are grateful to Dr. Natasha Zachara for providing a generous sample of mannosamine, and for helpful comments.

REFERENCES

1. Mildvan, A. S., Xia, Z., Azurmendi, H. F., Saraswat, V., Legler, P. M., Massiah, M. A., Gabelli, S. B., Bianchet, M. A., Kang, L.-W., and Amzel, L. M. (2005) Structures and mechanisms of Nudix hydrolases, *Arch. Biochem. Biophys. 433*, 129−143.
2. Frick, D. N., Townsend, B. D., and Bessman, M. J. (1995) A novel GDP-mannose mannosyl hydrolase shares homology with the MutT family of enzymes, *J. Biol. Chem. 270*, 24086−24091.
3. Lin, J., Abeygunawardana, C., Frick, D. N., Bessman, M. J., and Mildvan, A. S. (1997) Solution structure of the quaternary MutT-M^{2+}-AMPCPP-M^{2+} complex and mechanism of its pyrophosphohydrolase action, *Biochemistry 36*, 1199−1211.
4. Legler, P. M., Lee, H. C., Peisach, J., and Mildvan, A. S. (2002) Kinetic and magnetic resonance studies of the role of metal ions in the mechanism of *E. coli* GDP-mannose mannosyl hydrolase, an unusual Nudix enzyme, *Biochemistry 41*, 4655−4668.
5. Legler, P. M., Massiah, M. A., and Mildvan, A. S. (2002) Mutational, kinetic, and NMR studies of the mechanism of *E. coli* GDP-mannose mannosyl hydrolase, an unusual Nudix enzyme, *Biochemistry 41*, 10834−10848.
6. Gabelli, S. B., Bianchet, M. A., Azurmendi, H. F., Xia, Z., Saraswat, V., Mildvan, A. S., and Amzel, L. M. (2004) Structure and mechanism of GDP-mannose glycosyl hydrolase, a Nudix enzyme that cleaves at carbon instead of phosphorus, *Structure 12*, 927−935.
7. Legler, P. M., Massiah, M. A., Bessman, M. J., and Mildvan, A. S. (2000) GDP-mannose hydrolase catalyzes nucleophilic substitution at carbon, unlike all other Nudix enzymes, *Biochemistry 39*, 8603−8608.
8. Gabelli, S. B., Bianchet, M. A., Ohnishi, Y., Ichikawa, Y., Bessman, M. J., and Amzel, L. M. (2002) Mechanism of the *Escherichia coli* ADP-ribose pyrophosphatase, a Nudix hydrolase, *Biochemistry 41*, 9279−9285.
9. Withers, S. G. (2001) Mechanism of glycosyl transferases and hydrolases, *Carbohydr. Polym. 44*, 325−337.
10. Vasella, A., Davies, G. J., and Böhm, M. (2002) Glycosidase mechanisms, *Curr. Opin. Chem. Biol. 6*, 619−629.
11. Guérin, D. M. A., Lascombe, M.-B., Costabel, M., Souchon, H., Lamzin, V., Béguin, P., and Alzari, P. M. (2002) Atomic (0.94 Å) resolution structure of an inverting glycosidase in complex with substrate, *J. Mol. Biol. 315*, 1061−1069.
12. Cleland, W. W., and Henge, A. C. (1995) Mechanisms of phosphoryl and acyl transfer, *FASEB J. 9*, 1585−1594.
13. Mildvan, A. S. (1997) Mechanisms of signaling and related enzymes, *Proteins: Struct., Funct., Genet. 29*, 401−416.
14. Withers, S. G., Rupitz, K., and Street, I. P. (1988) 2-Deoxy-2-fluoro-D-glycosyl fluorides: A new class of specific mechanism-based glycosidase inhibitors, *J. Biol. Chem. 263*, 7929−7932.
15. Burkart, M. D., Vincent, S. P., Düffels, A, Murray, B. W., Ley, S. V., and Wong, C.-H. (2000) Chemo-enzymatic synthesis of fluorinated sugar nucleotide: Useful mechanistic probes for glycosyltransferases, *Bioorg. Med. Chem. 8*, 1937−1946.
16. Xia, Z., Azurmendi, H. F., Gabelli, S. B., Bianchet, M. A., Amzel, L. M., and Mildvan, A. S. (2004) Structural and mutational evidence for a dissociative mechanism in the reaction catalyzed by GDP-mannose mannosyl hydrolase (GDPMH), Poster BIOL-108, 228th National Meeting of the American Chemical Society, Philadelphia, PA, Aug 22−26, 2004.
17. Stick, R. V., and Watts, A. G. (2002) The chameleon of retaining glycoside hydrolases and retaining glycosyl transferases: The catalytic nucleophile, *Monatsh. Chem. 133*, 541−554.
18. Wong, C.-H., and Hayashi, T. (1998) Process for preparing nucleotide inhibitors of glycosyltransferases, U.S. Patent 5,770,-407; WO Patent 98/25940.
19. Gill, S. C., and von Hippel, P. H. (1989) Calculation of protein extinction coefficients from amino acid sequence data, *Anal. Biochem. 182*, 319−326.
20. Saraswat, V., Azurmendi, H. F., and Mildvan, A. S. (2004) Mutational, NMR, and NH exchange studies of the selective binding of 8-oxo-dGMP by the MutT pyrophohydrolase, *Biochemistry 43*, 3404−3414.
21. Mahuren, J. D., Coburn, S. P., Slominski, A., and Wortsman, J. (2001) Microassay of phosphate provides a general method for measuring the activity of phosphatases using physiological non-chromogenic substrates such as lysophosphatidic acid, *Anal. Biochem. 298*, 241−245.
22. Czerwinski, R. M., Johnson, W. H., Whitman, C. P., Harris, T. K., Abeygunawardana, C., and Mildvan, A. S. (1997) Kinetic and structural effects of mutations of the catalytic amino-terminal proline in 4-oxalocrotonate tautomerase, *Biochemistry 36*, 14551−14560.
23. Mildvan, A. S., Weber, D. J., and Kuliopulos, A. (1992) Quantitative interpretations of double mutations of enzymes, *Arch. Biochem. Biophys. 294*, 327−340.
24. Mildvan, A. S. (2004) Inverse thinking about double mutants of enzymes, *Biochemistry 43*, 14517−14520.
25. Jensen, H. H., Lyngbye, L., Jensen, A., and Bols, M. (2002) Stereoelectronic substituent effects in polyhydroxylated piperidines and hexahydropyridazines, *Chem.—Eur. J. 8*, 1218−1226.
26. Dixon, M., Webb, E. C., Thorne, C. J. R., and Tipton, K. F. (1979) *Enzymes*, 3rd ed., p 163, Academic Press, New York.
27. Brooks, B. R., Bruccoleri, R. E., Olafson, B. D., States, D. J., Swaminathan, S., and Karplus, M. (1983) CHARMM: A program for macromolecular energy, minimization and dynamics calculations, *J. Comput. Chem. 4*, 187−217.
28. Withers, S. G., MacLennan, D. J., and Street, I. P. (1986) The synthesis and hydrolysis of a series of deoxyfluoro-D-glucopyranosyl phosphates, *Carbohydr. Res. 154*, 127−144.
29. Zechel, D. L., and Withers, S. G. (2000) Glycosidase mechanisms: Anatomy of a finely tuned catalyst, *Acc. Chem. Res. 33*, 11−18.
30. Wolfenden, R., Lu, X., and Young, G. (1998) Spontaneous hydrolysis of glycosides, *J. Am. Chem. Soc. 120*, 6814−6815.
31. Percival, M. D., and Withers, S. G. (1992) Binding energy and catalysis: Deoxyfluoro sugars as probes of hydrogen bonding in phosphoglucomutase, *Biochemistry 31*, 498−505.
32. Watts, A. G., Damager, I., Amaya, M. L., Buschiazzo, A., Alzari, P., Frasch, A. C., and Withers, S. G. (2003) *Trypanosoma cruzi* trans-sialidase operates through a covalent sialyl-enzyme intermediate: Tyrosine is the catalytic nucleophile, *J. Am. Chem. Soc. 125*, 7532−7533.
33. Burmeister, W. P., Cottaz, S., Rollin, P., Vasella, A., and Henrissat, B. (2000) High-resolution X-ray crystallography shows that ascorbate is a cofactor for myrosinases and substitutes for the function of the catalytic base, *J. Biol. Chem. 275*, 39385−39393.
34. Burmeister, W. P., Cottaz, S., Driguez, H., Iori, R., Palmieri, S., and Henrissat, B. (1997) The crystal structures of *Sinapis alba* myrosinase and a covalent glycosyl-enzyme intermediate provide insights into the substrate recognition and active-site machinery of an S-glycosidase, *Structure 5*, 663−675.

BI050583V